FULL PAPER

Structural and Photophysical Characterization of All Five Constitutional Isomers of the Octaethyl-β,β'-dioxo-bacterio- and -isobacteriochlorin Series

Christian Brückner,*[a] Nivedita Chaudhri,[a],& Dustin E. Nevonen,[b],& Sayantan Bhattacharya,[c] Arthur Graf,[c] Elizabeth Kaesmann,[a] Ruoshi Li,[a] Matthew J. Guberman-Pfeffer,[a] Tomoyasu Mani,[a] Arunpatcha Nimthong-Roldán,[d] Matthias Zeller,[d],[e] Adrien A. P. Chauvet,[c] and Victor Nemykin*[b],[f]

[a] Prof. Dr. C. Brückner, Prof. Dr. T. Mani, Dr. N. Chaudhri, Dr. R. Li, Dr. M.J. Guberman-Pfeffer, E. Kaesmann
Department of Chemistry
University of Connecticut
Storrs, CT 06269-3060, United States
E-mail: c.bruckner@uconn.edu
Homepage: http://bruckner.research.uconn.edu

[b] D.E. Nevonen, Prof. Dr. Nemykin
Department of Chemistry
University of Manitoba
Winnipeg, Manitoba R3T 2N2, Canada

[c] Dr. A.A.P. Chauvet, Dr. S. Bhattacharya, A. Graf,
Department of Chemistry
University of Sheffield
Dainton Building
Sheffield S3 7HF, United Kingdom

[d] Dr. A. Nimthong-Roldán, Dr. M. Zeller
Department of Chemistry
Youngstown State University
One University Plaza
Youngstown, OH 44555-3663, United States

[e] Current address: Dr. M. Zeller
Department of Chemistry
Purdue University
560 Oval Drive
West Lafayette, IN 47907-2084, United States

[f] Prof. Dr. V. Nemykin
Department of Chemistry
University of Tennessee
552 Buehler Hall, 1420 Circle Dr.
Knoxville, TN 37996-1600, United States
E-mail: vnemykin@utk.edu

& Contributed equally

Supporting information (ESI) for this article is given via a link at the end of the document.

Abstract: It is well-known that treatment of β-octaethylporphyrin with H_2O_2/conc. H_2SO_4 converts it to the corresponding β-oxochlorin as well as all all five isomers of the β,β'-dioxo derivatives: two bacteriochlorin-type isomers (β-oxo groups at opposite pyrrolic building blocks) and three isobacteriochlorin-type isomers (β-oxo-groups at adjacent pyrrolic building blocks). By virtue of the presence of the strongly electronically coupled β-oxo auxochromes, none of the chromophores are archetypical chlorins, bacteriochlorins, or isobacteriochlorins. We firstly present here, inter alia, the single crystal X-ray structures of all free-base diketone isomers and a comparative description of their UV-vis absorption spectra in neutral and acidic solutions, fluorescence emission properties and singlet oxygen photosensitization properties, Magnetic Circular Dichroism (MCD) spectra, and singlet excited state lifetimes. DFT computations uncover underlying tautomeric equilibria and the electronic interactions controlling their electronic properties, adding to the understanding of porphyrinoids carrying β-oxo functionalities. This comparative study lays the basis for their further utilization.

Introduction

All naturally occurring tetrapyrrolic macrocycles, the 'pigments of life', carry alkyl substituents at their β-pyrrolic positions.[1] While β-octaalkylporphyrins and -chlorins, such as protoporphyrin IX or the chlorophylls, are readily available in quantity from slaughterhouse wastes[2] or plant sources,[3] respectively, their derivatization is hampered by regioselectivity problems. Thus, total syntheses and semi-syntheses of β-alkylhydroporphyrins were developed by the groups of Battersby, Eschenmoser, Montforts, Kishi, Smith, Jacobi, Scherz, Lindsey, and others.[4] Particularly the methodologies adapted or developed over the past decade by Lindsey and co-workers made the efficient total syntheses of (functionalized) β-alkylhydroporphyrins feasible with unprecedented flexibility with respect to the number, type, and arrangement of the β- and *meso*-substituents that can be established,[4i-k] including β-oxo-functionalities.[5] Irrespective of this progress, these syntheses remain non-trivial. β-Octaethylporphyrin (**OEP**) remains the most readily accessible

synthetic β-alkylporphyrin;[6],[7] its symmetry simplifies its functionalization.[8]

The introduction of β-oxo functionalities into the porphyrinic chromophore strongly affects its electronic properties.[5a, 5c, 9] For example, Lindsey and co-workers synthesized a series of mono- and dioxochlorins, such as 7,17-dioxobacteriochlorin **1**, and studied the auxochromic effects of the oxo-functionality.[5] The electronic structure of the potent singlet oxygen photosensitizer **1**[10] was characterized as a red-shifted chlorin — and not a typical bacteriochlorin as the substitution pattern might suggest.[5b] We found that the octaethyl-7,17-dioxobacteriochlorin framework is less basic and more difficult to metallate when compared to the corresponding oxochlorin or porphyrin.[9f]

The strong electronic influences of the β-oxo-functionalities are also reflected in the porpholactones, such as when comparing the properties of the isomers **2**^{7,17} and **2**^{7,18},[11] or the members of the isobacteriochlorindilactone series.[11c, 11d] Furthermore, work by the groups of Shen, Sessler, and Zhang on the aromaticity differences between reduced bacteriochlorindilactone isomers demonstrated the profound and frequently unexpected electronic influences of the β-oxo-functionalities.[12]

β,β'-Dioxochlorin chromophores are also found in nature. For example, a 2,7-dioxoisobacteriochlorin framework is found in heme d_1 (**3**), the prosthetic group in microbial nitrite reductases.[13] A 7,17-dioxobacteriochlorin chromophore is the basis of tolyporphin A (**4**), one member of a family of green tetrapyrrolic pigments isolated from a cyanobacterium-microbial ecological unit of unknown function, but endowed with intriguing medicinal properties.[14] Model systems for both chromophores were studied.[5b, 9f, 15]

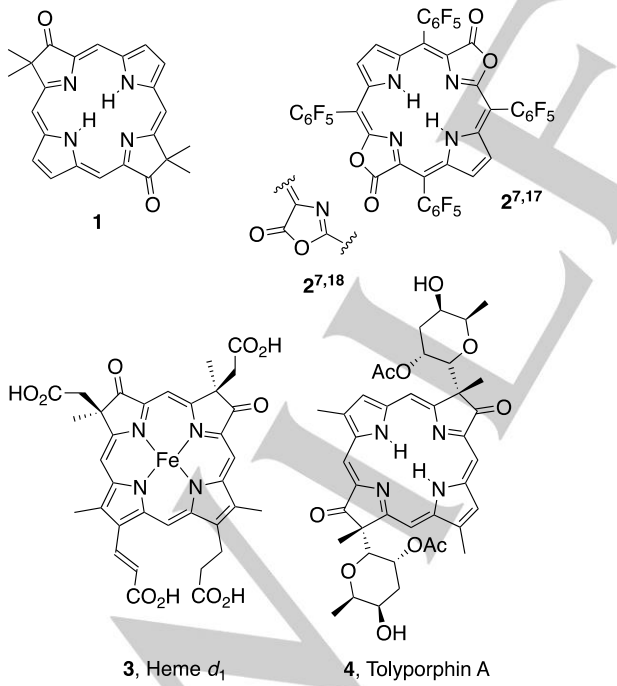

Figure 1. Literature-known β,β'-dioxo-substituted porphyrinoids.

The simplest synthetic methodology that introduces β-oxo functionalities into β-alkylporphyrins is their treatment with H_2O_2 in conc. H_2SO_4. The reaction harkens back to studies by the group of Fischer in the 1930's, albeit the reaction products were not correctly identified at the time.[16] The true connectivity of the major product oxochlorin **5** as the result of the treatment of **OEP** with H_2O_2/H_2SO_4 was identified in 1964 by the group of Johnson (Scheme 1).[17] The chromatographic separation of all products formed in reaction of **OEP** by the group of Inhoffen and later Chang allowed the isolation and identification of oxochlorin **5** and all isomers of the diketones: the three possible isomers of the dioxoisobacteriochlorin series **6** to **8**, the two isomers of the dioxobacteriochlorin series **9** and **10**, as well as triketone pyrrocorphins, *meso*-oxo-substituted phlorins, and ring-opened products.[18] We focus here exclusively on oxochlorin **5** and the isomers of the dioxoderivatives **6** through **10**.

The oxochlorins were likely formed along single and double epoxidation → epoxide opening by water → pinacol-pinacolone rearrangement of the resulting *trans*-diol pathways.[17] None of the intermediates were observed. However, chlorin *cis*-diol **11** can be prepared independently and shown by Chang and co-workers to be susceptible to a pinacol-pinacolone rearrangement, forming oxochlorin **5**.[19] The applicability of the H_2O_2/H_2SO_4 reaction to other porphyrins than **OEP** was also demonstrated.[18b, 20]

The chemical properties of the OEP-derived oxochlorins — primarily that of oxochlorin **5** — with respect to reduction,[21] carbonyl *C*-methylation,[18b] *N*-methylation,[22] *meso*-deuteration,[23] osmylation,[24] and thionation[25] reactions were studied. We also found oxochlorin **5** to be a starting material for the preparation of a pyrrolinone-expanded product.[8h, 26] The group of Stolzenberg, and others, studied the metal complexes of **5** (specifically, their Co(II),[27] Ni(II), Cu(II),[28] Zn(II), Al(III)(OH), Mg(II), and Fe(III)Cl[29] complexes).[21a, 30] The Pt(II) complex of **5** was used as an optical oxygen sensor.[31] We reported the reactivity of the free-base and Ni(II) complex of oxochlorin **5**, their oximes,[8h] the free-base *N*-oxide,[8b] and *meso*-chlorides.[8c] Fewer studies of the dioxochlorins were published, but a low-resolution structure of free-base dioxobacteriochlorin **9** is known;[25] we recently studied the insertion of Co(II), Ni(II), Cu(II), Zn(II), Pd(II), Ag(II), Cd(II), and Fe(III) into **9** and determined the solid-state structures of its Ni(II), Cu(II), Pd(II), and Ag(II) comple–xes.[9f] Likewise, the Ni(II),[32] Co(II),[27] Fe(III),[15a] and Cu(II)[15] complexes of dioxoisobacteriochlorin isomer **6** were described.

Thus, oxochlorin **5** and at least some of the dioxochlorin isomers were not left entirely unexplored in the 50 years since their discovery. Nonetheless, provided that β-oxochlorin **5** and all isomers of the β,β'-dioxochlorins can be prepared in a single step from a commercially available starting material, it is surprising that no detailed comparative study of their structures and electronic properties was reported to date. This account closes this gap.

We thus report the single crystal X-ray structures of all free-base diketone isomers, their optical properties (UV-vis absorption spectra in neutral and acidic solutions, fluorescence emission properties, including quantum yields and singlet state lifetimes, and MCD spectra), as well as their singlet oxygen ($^1O_2$) photosensitization properties. We included **OEP** and β-oxochlorin **5** as benchmarks. DFT computations help to derive an understanding of the underlying tautomeric equilibria and electronic effects controlling these properties. In so doing, we define more clearly the effects the number and particularly distribution of the β-oxo-substituents around the ring have on the electronic properties of these β,β'-dioxoporphyrinoids.

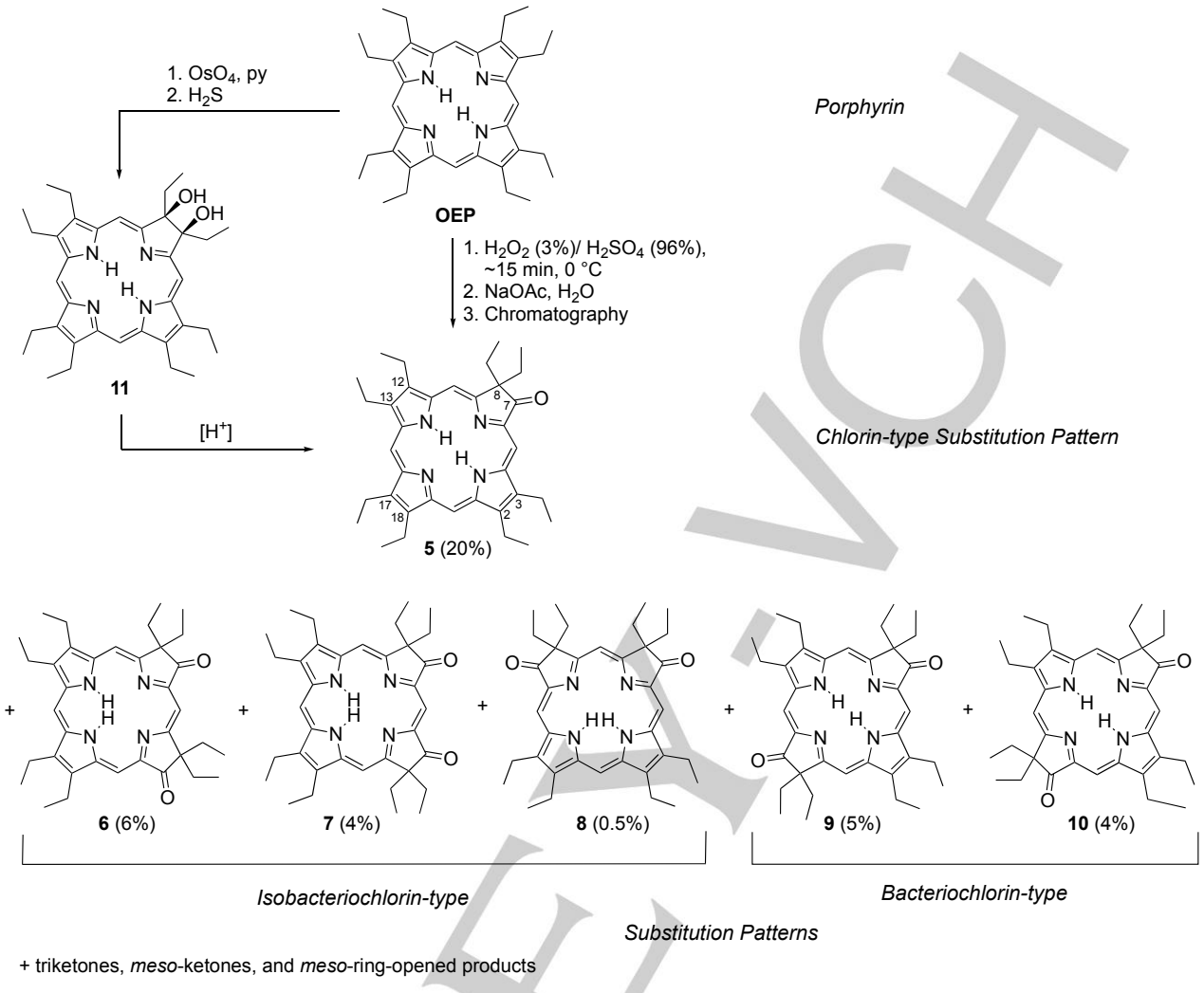

Scheme 1. Oxidation of **OEP** to the corresponding β-oxochlorin, β,β'-dioxoisobacteriochlorin-, and β,β'-dioxobacteriochlorin-type isomers.[17a, 18a, 18b] Shown also is the numbering system used to formally name the (di)oxochlorins.

Results and Discussion

Oxochlorin Syntheses

The syntheses of the β-oxochromophores **5** through **10** from **OEP** proceeded as principally described by Inhoffen,[18a, 18c] and later Chang:[18b] **OEP** (in 2-5 g batches) was reacted in 96% H_2SO_4 (200-500 mL) with a large stoichiometric excess of 3% H_2O_2 at ice temperatures (< 5 °C) over the course of about 15 min, at which point the starting material was near-quantitatively converted. Column chromatography allowed the isolation of, in order of increasing polarity, first oxochlorin **5** (pink), followed by a mixture of dioxochlorins **9**, **8**, and **10**, and then in distinct bands **6** (greenish purple), and finally **7** (light green); subsequent preparative plate chromatography or automated medium pressure chromatography separated dioxochlorins **9** (purple), **8** (blue), and **10** (brown) from each other. The yields, UV-vis, and ^{1}H NMR spectroscopic data of the products were in close agreement with those reported in literature.[18a, 18b] We acquired an expanded set of spectroscopic data of the compounds, including ^{13}C NMR, ^{1}H,^{1}H-COSY and HSQC spectra, to further characterize the compounds and to provide a basis for their further derivatization.[33] Specifically, the HSQC spectra correlated the carbonyl carbon signals to the neighboring β- or α-pyrrolic (between 130 to 165 ppm) and *meso*-carbons (between 85 to 105 ppm); for details and a reproduction of the spectra, see ESI.

Decreasing the acid concentration from 96% to 80% in 4% increments (temperatures all held at < 5 °C) slowed the reaction rate, concomitant with the reduction in yields of the 'over-oxidized' products (ring-opened products, triketones, oxo-phlorins). However, the formation of the desired oxo- and dioxochlorins was also suppressed, with the rare products (such as **8** and **10**) not being formed at all below 96 and 85% H_2SO_4, respectively. At 80% H_2SO_4, only traces of oxochlorin **5** are formed. The replacement of H_2O_2 by 3 equiv $K_2S_2O_8$ (based on the amount of **OEP**) is possible and led to a slightly reduced yield of 2,7-dioxoisobacteriochlorin **6** (4%) but furnished an increased yield (up to 2%) of 7,17-dioxobacteriochlorin **10**. We could find no other advantage of using this oxidant. For further details, see ESI.

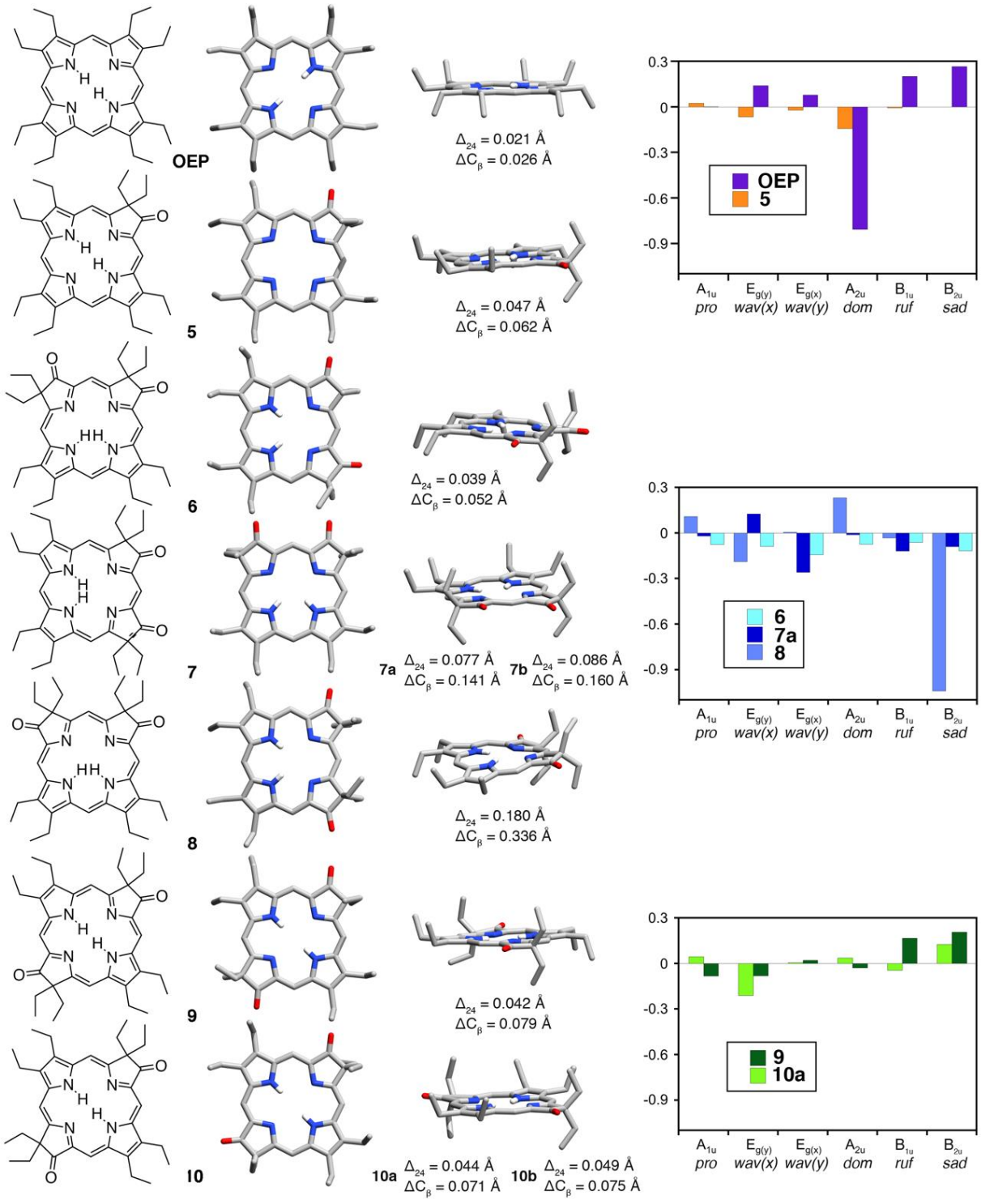

Figure 2. Stick presentations of the molecular structures of compounds indicated, top (left column) and oblique (middle column) views. All hydrogen atoms except when bound to N, disorder, and solvent, when present, were omitted for clarity; when present only one representative molecule of two non-equivalent molecules in the crystal is shown. The Δ_{24} values listed are root-mean-square values of the deviation from planarity of the $C_{20}N_4$ macrocycle $\sqrt{\frac{1}{24}(x_1^2 + x_2^2 + \ldots + x_{24}^2)}$, i.e. omitting the β-oxygen atoms from that determination; the ΔC_β values similarly indicate the deviation of the eight β-pyrrolic carbon atoms from the mean plane. Normal mode Structural Decomposition (NSD) analysis of the chromophore conformations (right column).[34] For details to the structural determinations, see ESI. Structures of **OEP**[35] and **5**[8h] were reported previously and are included for comparison; all other this work.

Since the combined yields of products **6**, **7**, plus **8** and products **9** plus **10**, respectively, are essentially the same, the introduction of a second oxo-functionality to **5** is not subject to any (major) regioselectivity with respect to the formation of isobacterio- versus

bacteriochlorin-type chromophores. This distinguishes this reaction from many other reactions that convert chlorins to either bacterio- or isobacteriochlorins.[36] We attribute the absence of the typical regioselectivity of the conversion of chlorins to the fact that the reactions take place under extremely acidic conditions on the protonated chromophores.

There are, however, some differences in the formation among the relative quantities of the five individual dioxoisomers. Four of the five dioxo-regioisomers are formed in comparable yields; the slight differences of their isolated yields likely reflect as much the different degrees of difficulty of their chromatographic isolation as intrinsic reactivity differences — with one exception: 7,13-Dioxoisobacteriochlorin **8** is formed in about an order of magnitude lower yield than all other isomers. It is also the only isomer in which two *gem*-diethyl groups face each other. However, the computed heats of formation of all five dioxo-isomers suggest that this arrangement of the two *gem*-diethyl groups introduces no steric strain into the molecule (Table 1). While the bacteriochlorins are generally more stable than the isobacteriochlorin series – an effect likely linked to the greater steric strain between the inner NH hydrogen atoms in the *adj*-tautomers of the isobacteriochlorins (for a more detailed discussion, see below), isomer **8** does not have a higher heat of formation than any of the other dioxoisobacteriochlorin isomers.

The findings of the occurrence of different amounts of the isomers are comparable to, for example, the dynamics of the formation of the *meso*-tetraarylporphodilactone regioisomers, though here some electronic and steric effects could be deduced to play a role.[11c, 37]

Table 1. Relative heats of formation (ΔH_f) of the compounds indicated (in their most stable tautomeric form; cf. to Figure 4).

Compound	Relative Heats of Formation (ΔH_f)[a] [kJmol^{-1}]
6ad	6.1
7ad	7.2
8ac	5.5
9ac	0.4
10ac	0.0[b]

[a] Conformation computed using M06/6-311+G(d,p), most stable tautomer, re-optimized with the BHandHLYP/def2SVP method; for details to the computations, see ESI. [b] By definition; reference compound.

β,β'-Dioxochlorin X-Ray Single Crystal Structures

X-ray diffraction-quality single crystals could be grown for all oxochlorin isomers by vapor diffusion techniques, confirming their spectroscopically assigned connectivity (Figure 2). Like the conformation of the parent porphyrin **OEP**,[35] most are idealized planar, with only minor deviations spread over many of the principle out-of-plane deformation modes,[38] with one notable exception: Dioxoisobacteriochlorin **8** possesses a modest but notable saddling (B_{2u} normal coordinate) distortion.

Porphyrin **OEP**, oxochlorin **5**, and dioxobacteriochlorin isomers **9** and **10** are, as expected, present in the tautomeric form that places the NH hydrogen atoms at opposite positions on pyrrole moieties; also as expected, the dioxoisobacteriochlorin isomers **6** through **8** are, present in the tautomeric form that places the NH hydrogen atoms on the adjacent pyrroles.[39] The computational and spectroscopic data presented below will present a more refined picture of the tautomers present in solution.

The introduction of the oxo- and *gem*-diethyl moieties do, on their own, impose no major steric demands on the macrocycle. Oxochlorin **5** is, in fact, more planar than **OEP**, that exhibits a slight doming (A_{2u} normal coordinate) deformation. We rationalize the deviation from planarity of dioxoisobacteriochlorin isomer **8** by the presence of the two *gem*-diethyl moieties facing each other. This arrangement induces a slight conformational restraint into the macrocycle that then exacerbates the steric clash of the adjacent NH groups by preventing effective evasion. Note that both NH-carrying pyrroles are tilted into the same hemisphere, whereas in the other molecules they are pointing into opposing hemispheres.

UV-vis Absorption and Fluorescence Emission Properties

The UV-vis absorption spectra of oxochlorins **5** through **10**, and the benchmark porphyrin **OEP**, in neutral and protonated (in the presence of TFA) forms, and their fluorescence emission spectra in the neutral form are shown in Figure 3 (data tabulated in Table 2).

All spectra of the neutral chromophores are typical for porphyrinoids (strong Soret band with a number of Q-bands) and are as described before,[18a, 18b] but a number of observations are notable. Oxochlorin **5** derives its name from its chlorin-like UV-vis spectrum (strongest absorbing Q-band is the λ_{max} band); it also exhibits a chlorin-typical single emission band. The spectra of the dioxo-isobacteriochlorin and -bacteriochlorin families are clearly differentiated from each other, as are the spectra of each isomer within a family, highlighting the strong electronic influence of the oxo-functionality on the chromophore. This is not unlike the effects of the carbonyl groups in the porphodilactones.[11] The spectrum of the 7,17-dioxochromophore (such as present in compound **9**) was shown to be more chlorin- than bacteriochlorin-like.[5b] Upon first inspection, this can also be said for its isomer **10**. The spectra of the isobacteriochlorin family (**6**, **7**, and **8**) appear to be more typically isobacteriochlorin-like.[40]

The single major band fluorescence spectra showing the porphyrinoid-typical small Stokes shift (10-11 nm for the dioxoisobacteriochlorin, and 1-2 nm for the dioxobacteriochlorin series) are all hydroporphyrin-like, with one exception: Dioxoisobacteriochlorin isomer **7** shows a strong two-band spectrum. Computations presented below (and fluorescence studies, see ESI) will suggest the origin to lie in the presence of two tautomers of different optical properties.

The fluorescence quantum yields of all dioxochlorins investigated (in CH_2Cl_2) range between 12.5 and 17.1%, not varying much from those of oxochlorin **5** (16.1%) or **OEP** (14.4%) (Table 2).

The relative positions of the protonated spectra with respect to the corresponding spectra of the neutral species vary broadly; the Soret bands of the protonated species could be red- (e.g., for **OEP** and dioxoisobacteriochlorin isomer **7**) or blue-shifted (e.g., for oxochlorin **5**), or remain essentially unshifted (for dioxoiso-bacteriochlorin isomer **8**). Likewise, the shifts of the λ_{max} bands upon protonation show no unified trends, even within a chromophore class, and could be red- (e.g., for dioxoisobacterio–chlorin isomer **7**) or blue-shifted (e.g., for both dioxo-bacteriochlorin isomers **9** and **10**), or remain largely unshifted (for dioxoisobacteriochlorin isomer **8**). The protonation behavior of compounds **5**, **9**, and **10** was studied before.[9f] Compared to the basicity of **OEP**, the basicity of oxochlorin **5** was shown to be reduced and linear Hill plots for its spectrophotometric protonation

could be derived.[9f] On account of the presence of the second oxo-functionality and their bacteriochlorin-like chromophore, the basicity of the dioxobacteriochlorins **9** and **10** was further reduced significantly and complex, multi-site protonation events were observed.[9f] Here, we did not characterize the degree of protonation, or the protonation sites, except that all protonated spectra were derived under conditions that assured full protonation.

A connection between the degree of aromaticity and the longest wavelength of absorption (λ_{max}) was derived in the porpholactone series.[12] We measured the degree of aromaticity as the spread of the chemical shifts between the *meso*- and inner NH protons ($\Delta\delta_{meso\text{-}NH}$) that are subject to the shielding and deshielding effects, respectively, by the diatropic ring current; we also computed this parameter (Table 2).

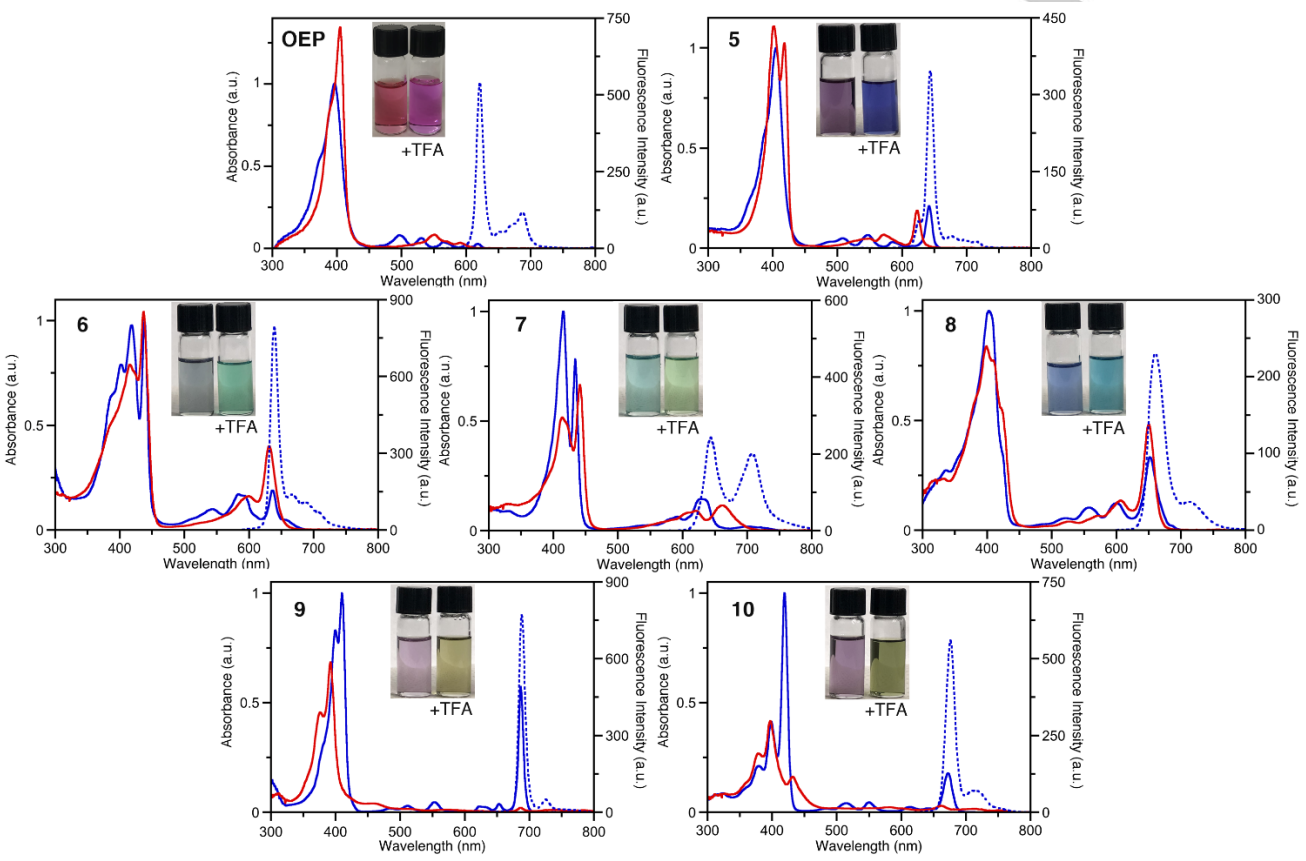

Figure 3. UV-vis (CH_2Cl_2, blue solid traces; CH_2Cl_2 + 0.41 M TFA, red solid traces) and fluorescence emission spectra (CH_2Cl_2, dotted blue trace) of the compounds indicated. $\lambda_{excitation} = \lambda_{Soret}$. Sufficient TFA was added to a sample recorded in blue to achieve full protonation, with dilution errors < 2%. The photographs display the colors of the samples in their neutral and protonated forms.

While the computed $\Delta\delta_{meso\text{-}NH}$ values are systematically about 3 ppm larger than the experimental values (except for dioxoisobacteriochlorin **8** that was computed as only one of two tautomers), the experimental trends are preserved. Among the dioxoisobacteriochlorins, only a weak correlation of λ_{max} and $\Delta\delta_{meso\text{-}NH}$ can be identified. While the compound with the longest λ_{max} (**7**, 699 nm) possesses the largest $\Delta\delta_{meso\text{-}NH}$, the two compounds with very similar λ_{max} values (**6**, 650 nm; **8**, 652 nm) exhibit much different $\Delta\delta_{meso\text{-}NH}$ values. Among the two dioxobacteriochlorins **9** and **10**, the predicted correlation between $\Delta\delta_{meso\text{-}NH}$ and λ_{max} holds.

Table 2. Photophysical data for dioxochlorins isomers **6**–**10** in comparison to those of **OEP** and oxochlorin **5**, in CH_2Cl_2, if not indicated otherwise. All data from this work, unless indicated otherwise.

	UV-vis (nm)[a]		Fluorescence Emission (nm) [rel. intensity]	Fluorescence Quantum Yield (%)[b]	Emission Lifetime τ_S (ns)	Radiative Rate K_f (s^{-1})	Singlet Oxygen $^1O_2$ ($^1\Delta_g$) Quantum Yield[c]	Average $\Delta\delta_{meso\text{-}NH}$ (ppm)	
	Soret-band(s) (nm) [log ε] ($M^{-1}cm^{-1}$)	Q-bands (nm) [log ε] ($M^{-1}cm^{-1}$)						Computed[d]	Experimental[e]
OEP	398 [5.11]	499 [4.09], 532 [3.93], 566 [3.75], 619 [3.63]	624 [1.00], 694 [0.22]	14.4	11.7 ± 0.02	7.3×10^7	0.66 ± 0.08	17.0	13.8
5	405 [5.03]	484 [sh], 508 [3.73], 546 [3.86], 585 [3.52], 641 [4.35]	644 [1.00], 674 [0.07], 714 [0.04]	16.1	5.3 ± 0.05	1.58×10^8	0.71 ± 0.04	15.6	12.6
6	402 [4.20], 418 [4.29], 438 [4.30]	543 [3.30], 583 [3.53], 636 [3.58], 650 (sh)	638 [1.00], 668 [0.25]	12.5	3.19 ± 0.107	2.74×10^8	0.66 ± 0.07	13.0	9.0
7	416 [4.93], 434 [5.06]	537 [sh], 592 [3.98], 630 [4.33], 699 [3.46]	643 [1.00], 707 [0.82]	14.1	1.55 ± 0.005	5.54×10^8	0.67 ± 0.05	13.9	10.8
8	405 [5.02]	519 [3.76], 557 [4.03], 599 [4.11], 652 [4.59]	667 [1.00], 716 [0.23]	17.1	2.44 ± 0.006	3.41×10^8	0.69 ± 0.14	7.8	6.7
9	400 [5.09], 410 [5.18]	483 [3.42], 511 [3.65], 553 [3.84], 622 [3.61], 653 [3.76], 686 [4.94]	688 [1.00], 725 [0.06]	14.6	3.31 ± 0.10	2.58×10^8	0.69 ± 0.04	15.6	12.0
10	378 [4.78], 399 [5.07], 419 [5.46]	482 [3.68], 513 [4.07], 549 [4.11], 612 [3.84], 640 [3.72], 672 [4.64]	675 [1.00], 718 [0.13]	15.6	2.65 ± 0.01	3.18×10^8	0.88 ± 0.16	13.5	11.0

[a] For UV-vis data in $CHCl_3$, see ESI or ref. [18a]. Sh = shoulder. [b] Reference compound *meso*-tetraphenylporphyrin.[41] [c] All in benzene, reference compound **OEP**: $^1O_2$ quantum yield 0.66 ± 0.08.[42] [d] Computed structures using conformation computed using M06/6-311+G(d,p), most stable tautomer; for details to the computations, see ESI. [d] From experimental section, see ESI.

Magnetic Circular Dichroism (MCD) **Spectroscopic Properties**

MCD spectroscopy was shown to be valuable to gain deeper insight into the classification of porphyrinic chromophores.[43] The MCD spectra of all oxo-derivatives are, next to the benchmark spectra of **OEP**, presented in Figure 4. In the case of oxochlorin **5**, the Q_x band is shifted from 618 nm in **OEP** to 642 nm with substantial growth in intensity. This band is associated with the negative MCD signal observed at 640 nm. The Q_y band in oxochlorin **5** is also shifted to lower energy (547 nm) compared to the Q_y band in **OEP** (530 nm). The Q_y band in oxochlorin **5** is associated with a strong, positive MCD signal centered at 545 nm. The Soret band in oxochlorin **5** was observed at 405 nm. Similar to the parent porphyrin **OEP**, the MCD spectrum of **5** has a complex structure in the Soret band region, which is dominated by a pair of positive-to-negative (in ascending energy) signals at 412 and 399 nm that form an MCD Faraday pseudo *A*-term.

The UV-vis and MCD spectra of dioxoisobacteriochlorins **6**-**8** are significantly more complex compared to those of the other chromophores considered here. The lowest energy *B*-term in the MCD spectrum of dioxoisobacteriochlorin isomer **6** (657 nm) has a negative amplitude and correlates well with the shoulder (at 658 nm) observed in its UV-vis spectrum; it furthermore is dominated by a pair of well-separated Faraday *B*-terms (at 637 and 581 nm), which correlate well with the bands observed at 636 and 583 nm in its UV-vis spectrum. Although the Soret bands in isomer **7** are also well-separated, both Q- and Soret band regions in the UV-vis spectrum of this compound are less complex than those in isomer **6**. More interestingly, a Faraday pseudo *A*-term (centered at 634 nm) dominates the MCD spectrum of dioxoisobacteriochlorin isomer **7**. The presence of such a pseudo *A*-term is rather unique among the dioxoisobacteriochlorins and can be rationalized on the basis of our DFT and TDDFT calculations presented below. Finally, the Soret band region in the UV-vis and MCD spectra of isomer **8** clearly consist of a large number of transitions, while four well-resolved bands observed in its Q-band region correlate well with MCD signals (at 667, 606, 550, and 521 nm).

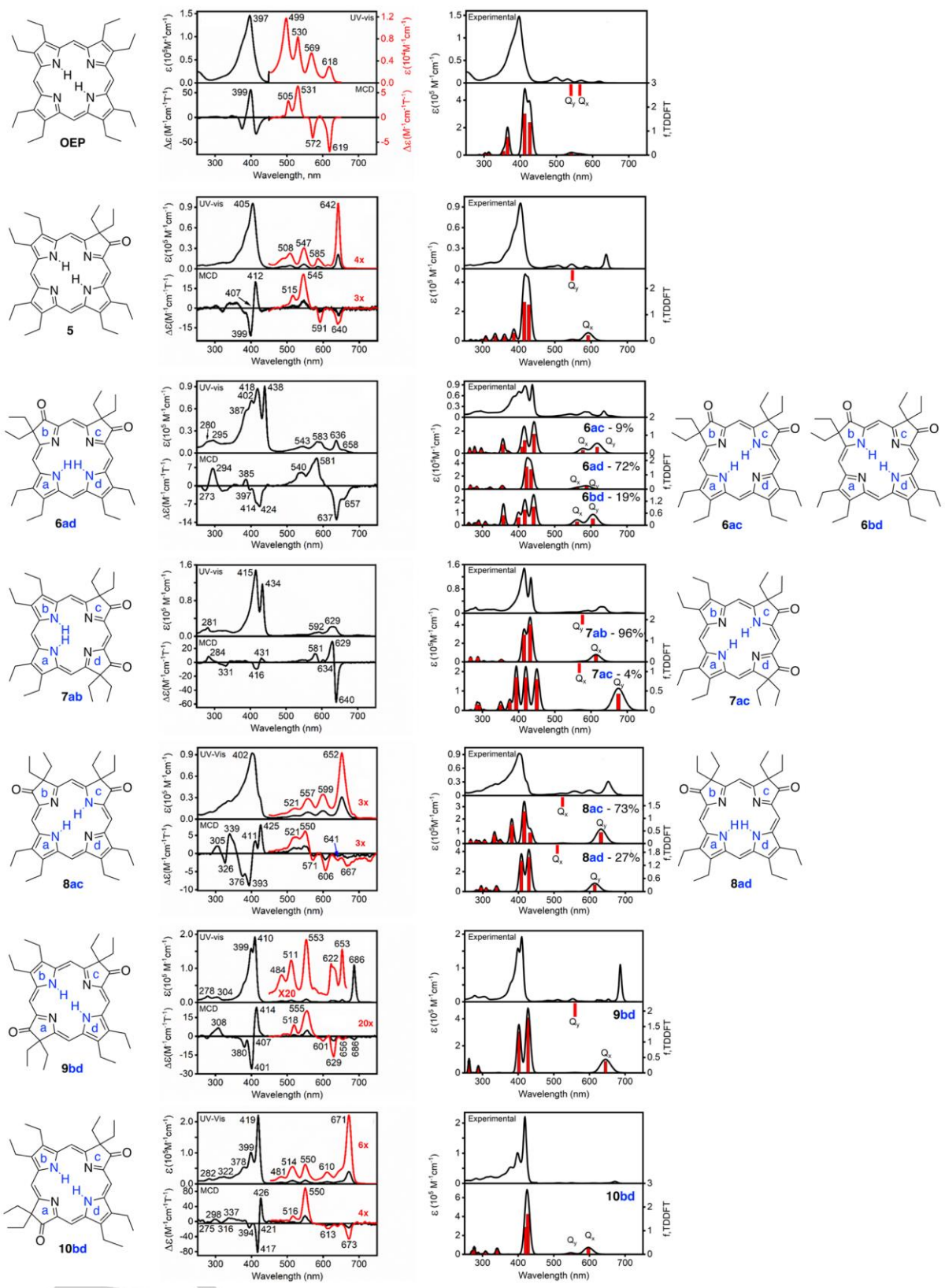

Figure 4. Left column of structures: The most stable tautomer considered. Left column of spectra: Experimental UV-vis and corresponding Magnetic Circular Dichroism (MCD) spectra (CH_2Cl_2) of the compounds indicated. Right column of spectra: Experimental (CH_2Cl_2) and TDDFT-simulated UV-vis absorption spectra of the major and minor tautomers indicated (and shown in the right column of structures), computed as the octamethyl derivatives. Tautomers considered and their room-temperature contribution to the spectra are shown, with the letters following the compound numbers indicating the presence of the NH hydrogen atom at pyrrolic rings a, b, c, or d, as shown.

The UV-vis and MCD spectra of dioxobacteriochlorins **9** and **10** are similar, but not identical. The intensity of the Q_x band dominates the Q-band region. The lowest energy Q_x band is observed at 686 nm for isomer **9** and at 671 nm for isomer **10** and both bands are associated with negative MCD signals. The Q_y bands of both dioxobacteriochlorins, at 553 and 550 nm, respectively, are associated with corresponding positive amplitude MCD *B*-terms centered at 555 and 550 nm, respectively. The Soret band in dioxobacteriochlorin **9** is centered at 410 nm and is associated with an MCD pseudo *A*-term, whereas the Soret band region for isomer **10** consists of three clear transitions (centered at 378, 399, and 419 nm); the most intense band at 419 nm is associated with an MCD pseudo *A*-term.

The energy differences between the Q_y and Q_x bands (i.e., also the lowest energy negative and positive MCD signals) in the Q-band region for the series of β-oxochromophores **5**-**10** varies between 273 and 3441 cm^{-1} and show no clear structural trends, although the largest Q_x-Q_y splitting are observed in dioxobacteriochlorins **9** and **10**. In the case of dioxoisobacteriochlorins **6**-**8**, Q_x-Q_y splitting varies between 273 and 3189 cm^{-1}. The lowest energy MCD signal for all compounds was always observed as an MCD *B*-term with a negative amplitude. This situation is typical for octa-alkyl- and *meso*-tetraaryl-porphyrins; it is indicative of the ΔHOMO being larger than the ΔLUMO (ΔHOMO is the energy difference between the a_{1u} and a_{2u} Gouterman's orbitals and ΔLUMO[43-44] is the energy difference between the e_g pair of Gouterman's orbitals, with the symmetry labels used for porphyrins in D_{4h} point group notation).[40, 45] This observation is quite unusual compared to some chlorins, isobacteriochlorins, and bacteriochlorins in which a reversed energy order was typically observed (associated with a positive MCD signal at lower energy and negative MCD signal at higher energy),[46] though some OEP-derived hydroporphyrins show also a similar sequence than observed here for compounds **5**-**10**.[46-47]

DFT Calculations – Tautomers

To rationalize the optical properties of the oxochlorins investigated, a series of DFT calculations using BP86 (GGA), MN12L (meta-GGA), TPSSh, and M06 (both hybrid) exchange-correlation functionals were conducted as it was expected that the predicted energies for the individual tautomers are dependent on the exchange-correlation functional chosen.[48] In the cases of oxochlorin **5** and dioxobacteriochlorins **9** and **10**, and in accord with the literature description of the preferred NH-tautomers of the chlorin and bacteriochlorin-type hydroporphyrins,[10, 11d, 39, 49] a single tautomer carrying the NH protons on opposite pyrrolic rings was found to be energetically highly favored. However, the cases of the dioxoisobacteriochlorins **6**-**8** are more complex and we find that several possible NH tautomers, each with its own optical signature (Figure 4), are close enough in energy to be in equilibrium with each other (Table 3).[11d, 39, 49] Only tautomers that were similar ($\leq$ 2.5 kcal/mol) in energy to the most stable conformation are shown and were taken into consideration in the modeling of the spectra, as only they could contribute > 2% to the room-temperature UV-vis and MCD spectra.

Table 3. Dioxoisobacteriochlorin tautomers considered, their relative energies, and corresponding Boltzman distribution to the equilibrium mixture.

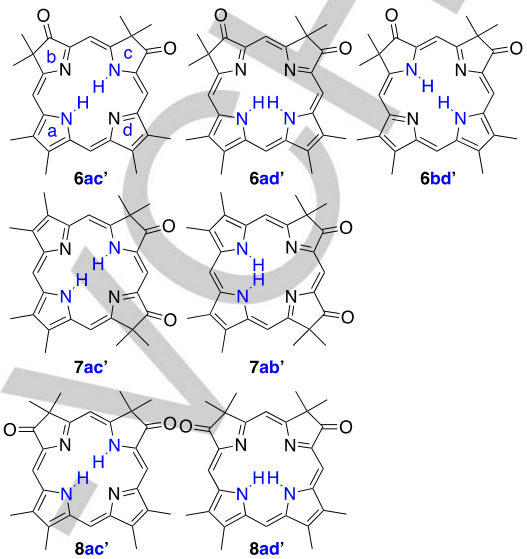

	Relative Energy (kcal/mol)			
Tautomer[a,b]	**BP86**	**MN12L**	**TPSSh**	**M06**
6ac'	1.01	1.03	1.39	1.26
6bd'	1.23	1.08	1.33	0.78
6ad'	0[c]	0[c]	0[c]	0[c]
7ac'	1.82	1.52	2.07	1.92
7ab'	0[c]	0[c]	0[c]	0[c]
8ac'	0.36	0[c]	0.26	0[c]
8ad'	0[c]	0.14	0[c]	0.59

[a] Because of the two-fold axial symmetry of compounds **7** and **8**, no further tautomers need to be considered. [b] Computed as the octamethyl derivatives **X'**. [c] By definition; reference compound in the isomer series **6**, **7**, and **8**, respectively.

The tautomers computed to be present balance the combination of sterically unfavorable arrangements of two NH hydrogen atoms on adjacent pyrroles with electronically favorable 'inner-inner-outer-outer' conjugation pathways (such as **6ad'** or **7ab'**) against the combination of sterically more favorable arrangements of both NH hydrogen atoms at opposite pyrroles with unfavorable electronics, i.e., forcing an 'inner' conjugation pathways through an NH nitrogen lone pair, such as in **6ac'** or **6bd'**).[39]

To our surprise, we found that the tautomeric preferences vary with the particular dioxoisobacteriochlorin isomers. In the cases of the dioxoisobacteriochlorins **6** and **7**, the "adj" tautomers (**6ad'** and **7ab'**) are the most stable and energetically well-separated (>1 kcal/mol in most cases) from the "opp" tautomers (**6ac'**, **6bd'**, and **7ac'**). This prediction is consistent across all tested functionals (Table 2). The energy difference between tautomers

8ac' and **8ad'** was predicted to be significantly smaller using two functionals (BP86 and TPSSh), and predicting **8ad'** to be the lowest energy tautomer. The remaining two functionals (MN12L and M06) predicted **8ac'** to be the lowest energy tautomer. Below we will confirm that the UV-vis spectra of the NH tautomers of each specific dioxochlorin class are much different from each other. As a consequence, the UV-vis and MCD spectra of the oxochlorins need to be modelled as a superposition of all NH tautomers present at ambient temperature.

DFT Calculations – UV-Vis and MCD Spectra

The DFT-predicted frontier orbitals shapes and electron density distributions (Figure 5) as well as the molecular orbitals energy diagram (Figure 6) for the compounds of interest (computed as their octamethyl derivatives **X'**) in their most stable tautomeric form highlights the energetic differences between all β-oxohydroporphyrins. Similar to the parent free-base **OEP'**, the HOMO of all compounds **5'**-**10'** possesses Gouterman's "a_{1u}" character while the HOMO-1 has Gouterman's "a_{2u}" character (in D_{4h} point group notation). In all cases, the LUMO and LUMO+1 resemble Gouterman's "e_g" pair of molecular orbitals.[40, 45]

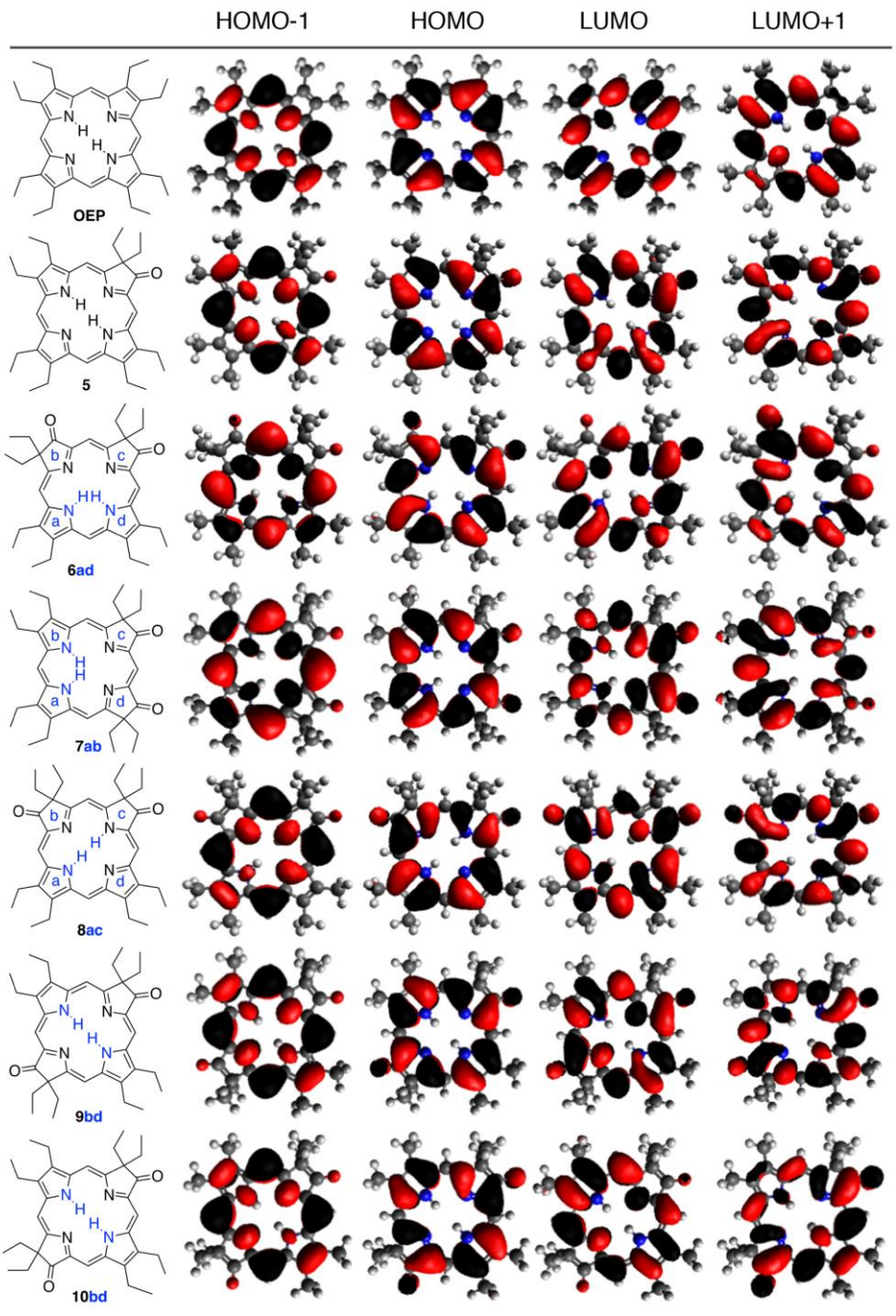

Figure 5. DFT-predicted (M06/6-311+G(d,p)) frontier molecular orbitals for the most stable tautomers of **OEP** and the oxochromophores **5** through **10**; computed as their octamethyl derivatives. For details, see ESI.

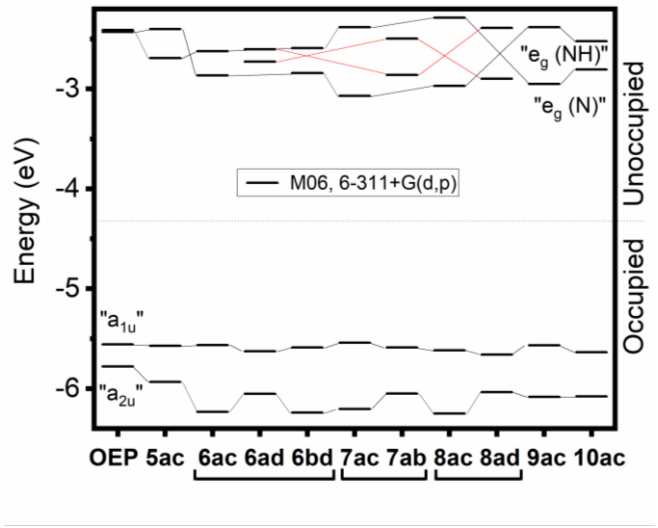

Figure 6. DFT-predicted energy level diagram for the most stable tautomers of **OEP'** and compounds **5'**-**10'**. Connectivity for the LUMO and LUMO+1 in *adj*-**6ad'**, **7ab'**, and **8ad'** is shown in red. Computed as their octamethyl derivatives **X'**. For details, see ESI.

Following the perimeter model,[43] one might expect that the negative to positive MCD signals with ascending energy will correlate with a ΔHOMO > ΔLUMO relationship (see also above). Except for four cases (**7ac'**, **8ac'**, **8ad'**, and **9'**; M06 functional), the DFT calculations predict a ΔHOMO > ΔLUMO relationship. This correlates well with their experimental MCD spectra (see ESI Table S3 for details). In the cases of dioxoisobacteriochlorins **7ac', 8ac',** and **8ad'**, the DFT calculations predicted the inverse ΔHOMO < ΔLUMO relationship, which was attributed to the observed reversed MCD signal sequence in the Q-band region (i.e. positive to negative MCD amplitudes for B-terms with ascending energy). According to the DFT calculations, however, the contribution of dioxoisobacteriochlorin tautomer **7ac'** is small (4%; M06 functional). Outliers aside, the cumulative experimental MCD spectra correlate well with the DFT calculations.

To correlate the experimental UV-Vis and MCD spectra with the DFT-predicted electronic structures of the target compounds, TDDFT calculations were performed on all of the systems (Figure 4). In the case of parent **OEP'**, the TDDFT-predicted UV-Vis spectrum confirms its expected correlation with Gouterman's four-orbital model, i.e., the Q-band region can be described by single electron excitations originating from the HOMO and HOMO-1 to the nearly degenerate LUMO and LUMO+1. Likewise, the energies and intensities of the Soret band region also fit Gouterman's model.

In the case of oxochlorin **5'**, the TDDFT calculations also predict that the first excited state is dominated by the HOMO to LUMO single electron excitation. Contrary to **OEP'**, however, the second excited state in the Q-band region of oxochlorin **5'** is predicted to be a superposition of almost equal HOMO to L-UMO+1 and HOMO-1 to LUMO single electron excitations (see ESI for details).

In the cases of dioxobacteriochlorins **9'** and **10'**, the TDDFT calculations predict that the first excited state is dominated by the HOMO to LUMO single electron excitations while the second excited state should consist of nearly equivalent excitations from HOMO to LUMO+1 and from HOMO-1 to LUMO.

The experimental UV-vis spectra of dioxobacteriochlorins **6'**-**8'** should be the superposition of the two or three NH tautomers that are in equilibrium with each other (at ambient temperature) (Table 2, Figure 4). In the case of dioxoisobacteriochlorin **6'**, the TDDFT-predicted spectra for *opp*-tautomers **6ac'** and **6bd'** are very similar to each other (~28% of the total contribution), while the TDDFT-predicted UV-vis spectrum of *adj*-tautomer **6ad'** (~72% of the total contribution) is quite different in the Q- and Soret-band regions. This explains the rather broad Q-band region and narrow Soret band region in the experimental UV-vis and MCD spectra of **6**. For all three tautomers, TDDFT calculations predict that the lowest-energy transition will be dominated by the HOMO→LUMO single-electron excitation and has y-polarization (the x-axis in **6ab'** was assumed to be parallel to the NH protons). We speculate that the *opp*-tautomers **6ac'** and **6bd'** are responsible for the lowest energy transition in the experimental UV-vis and MCD spectra of **6** (at 658 nm and 657 nm, respectively), while the more energetically favorable *adj*-tautomer **6ad'** forms the intense bands in the experimental UV-vis spectrum MCD spectra (at 636/583 nm and 637/581, respectively).

In the case of dioxoisobacteriochlorin **7**, DFT calculations predict that the *adj*-tautomer **7ab'** will contribute ~96% of the intensity to the UV-vis and MCD spectra of **7** (Table 2, Figure 4). Not surprisingly, the UV-vis and MCD spectra of **7** are significantly less complex than those of the multi-component spectra of **6**. Similar to *adj*-tautomer **6ad'**, TDDFT calculations predict much smaller (~2.8 times) Q_x-Q_y energy splitting in **7ab'** compared to that in **7ac'**. This could be the reason for the presence of the MCD pseudo *A*-term experimentally observed between 640 and 629 nm. More interestingly, polarization of the lowest energy band in **7ab'** is opposite to that in the **6ad'** and **8ad'** tautomers (Table 2).

In the case of dioxoisobacteriochlorin **8**, DFT predicts that its UV-vis and MCD spectra should be a superposition of the *adj*- and *opp*-tautomers **8ad'** (27%) and **8ac'** (73%), respectively. For both tautomers, TDDFT predicts that the Q_y band will have the lowest energy and will be dominated by the HOMO→LUMO single-electron excitation. The TDDFT-predicted Q_x transition has nearly equal contributions from the HOMO→LUMO+1 and HOMO-1→LUMO single-electron excitations.

Emission Lifetimes, Quantum Yields, and Singlet Oxygen Generation

The fluorescence quantum yields of all dioxochlorins did not very outside a range between 12.5 and 17.1 %, i.e., they lie broadly within the range found for oxochlorin **5** (16.1 %) and **OEP** (14.4 %) (Table 2). Thus, the differences between the various dioxochlorin isomers are generally smaller than some of the differences in the optical properties among the dilactone isomers.[11-12] In contrast, the emission lifetimes vary more broadly when comparing the lifetimes for **OEP** (11.7 ns), oxochlorin **5** (5.3 ns) with those of the dioxochlorins (ranging from 1.55 to 3.31 ns) (Table 2, Figure 7). Thus, their lifetimes show some structure-properties correlation as they generally decrease with the number of oxo-functionalities. Detailed investigations of the excited state dynamics of all dioxochlorins are underway.

The radiative rates for **OEP**, oxochlorin **5** and all dioxochlorins were calculated using the quantum yield (QY) and radiative lifetime and are tabulated in Table 2. The rates suggests a systematic 2-fold increase in the radiative relaxation rate with the addition of each β-oxo group over the rate for the benchmark compound **OEP**, i.e., a two-fold rate increase for 7-oxochlorin **5**

and ~4-fold increase for dioxo-bacterio/isobacteriochlorins (Figure 7).

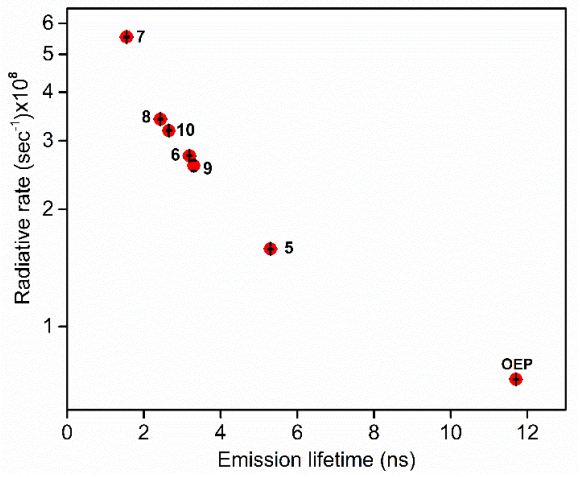

Figure 7. Graphical representation of radiative rate and emission lifetime for the oxoporphyrins investigated in comparison to the data for **OEP**.

Free-base porphyrins and hydroporphyrins are generally excellent photosensitizers for the conversion of triplet ($^3O_2$) to singlet ($^1O_2$) oxygen.[50] This is the basis for their utilization as photochemotherapeutics or in technical applications.[51] The singlet oxygen quantum yields measured for the dioxochlorins by direct emission of the singlet oxygen (in benzene) (Table 2) fall, with one exception, within a narrow range between 66 to 69% and are not much different from those of *meso*-tetraphenylporphyrin (63%) and oxochlorin **5** (66%). Only dioxobacteriochlorin isomer **10** is slightly higher (88%). The efficacy of the oxochlorins **5** to **10** to photo-generate singlet oxygen was also tested in DMF using the $^1O_2$ chemical trap 1,3-diphenylisobenzofuran (DPBF) (see ESI). Here, the dioxoisobacteriochlorin isomers were generally more efficient photosensitizers than **OEP**, though the dioxobacteriochlorin isomer **10** and oxochlorin **5** performed only slightly better than **OEP**, and dioxobacteriochlorin isomer **9** appeared to photodegrade the most rapidly.

Conclusion

We prepared the well-known β-oxochlorin **5** and all five isomers of the β,β'-dioxochlorins along known methodologies. We firstly presented their comprehensive comparative structural and spectroscopic characterization. Apart from the most strained isomer, all isomers are essentially planar. The electronic properties of the chromophores show the strong influences of the β,β'-dioxo-substituents in that, for example, none of the bacteriochlorin- or isobacteriochlorin-like architectures show bacteriochlorin- or isobacteriochlorin-type spectroscopic properties. All compounds are singlet oxygen sensitizers, some dioxoisobacteriochlorins even more so than the parent porphyrin **OEP**.

The performance of the TDDFT calculations to model the optical properties of the β-dioxochlorins is excellent overall. Indeed, the M06 calculations were able to reproduce all experimentally observed key features in the UV-vis and MCD spectra of all chromophores investigated. The TDDFT-predicted energies of the Q_x and Q_y bands were found to be within 0.1-0.15 eV without any artificial energy shifts, while the predicted Q_x-Q_y energy splitting also correlates very well with the experimental data. The more complex nature of the UV-vis and MCD spectra of isobacteriochlorins **6** and **8** could be confidently explained based on contributions from several NH tautomers, while the simpler spectral profile of **7** correlates well with the presence of only a single dominant NH tautomer and a different polarization of the lowest energy transition.

Thus, this contribution adds to the understanding of porphyrinoids carrying the β-oxo auxochrome. It further lays the foundation for the further utilization of these readily accessible β,β'-dioxo-derivatized porphyrinoid chromophores.

Experimental Section

Materials: Solvents and reagents were used as received. **OEP**[6] was converted to the oxochlorins using the procedure described by Inhoffen and Chang.[18a, 18b] For spectroscopic and analytical details of all compounds prepared, see ESI.

Aluminum-backed, silica gel 60, 250 μm thickness analytical plates, 20 × 20 cm, glass-backed, silica gel 60, 500 μm thickness preparative TLC plates, and standard grade, 60 Å, 32-63 μm flash column silica gel were used. Alternatively, flash column chromatography was performed on an automated flash chromatography system, on normal-phase silica gel columns.

UV-Vis and Fluorescence Measurements. UV-Vis data were obtained on Cary 100 or Jasco V-670 spectrophotometers in the solvents indicated.

Fluorescence Yields. Emission spectra were recorded on a FluroMax (Jobin-Yvon) spectrometer for quantum yield (ϕ) measurements. The fluorescence quantum yields (ϕ) were determined in CH_2Cl_2 relative to that of *meso*-tetraphenylporphyrin (ϕ = 0.13 in CH_2Cl_2).[41] Oxochlorins and reference compound were excited at 416 nm and emissions collected with gradually decreasing concentration to calculate ϕ.

Singlet Oxygen Yields. Steady-state $^1O_2$ phosphorescence spectra were recorded using an FLS1000 (Edinburgh), equipped with an extended red photomultiplier (PMT980) and InGaAs detector (spectral range 870 nm – 1650 nm). The singlet oxygen quantum yield of **OEP** (0.68 in benzene)[42] was used for the comparative determination of the quantum yields of the oxo-derivatives investigated.

Singlet State Lifetimes. Emission lifetimes were measured with the TCSPC technique using a Mini-Tau lifetime spectrometer (Edinburgh instruments).[52] Samples were dissolved in 1 cm quartz cuvette in CH_2Cl_2. TCSPC measurements were carried out by exciting the oxochlorins with a 410 nm NanoLed source with an instrument response function of ~300 ps.

MCD Spectroscopy. MCD data were obtained using a Jasco V-1500 spectropolarimeter (1.5 T electromagnet). Two spectra were recorded for each sample, one using a parallel field and the other using an antiparallel field. Spectral intensities were expressed as molar ellipticity per T.[53]

Computations. All DFT and TDDFT calculations were performed using the Gaussian 09 software.[54] The starting geometries for all compounds, computed as their octamethyl derivatives **X'**, were optimized using the BP86,[55] MN12L,[56] TPSSh,[57] and M06[58] exchange-correlation functionals. The equilibrium geometries were confirmed with the frequency calculations and more specifically, by the absence of imaginary frequencies. All atoms were modelled using the 6-311+G(d,p) basis set.[59] For the TDDFT calculations, the solvent effects were calculated using the PCM approach[60] with DCM as a solvent. The QMForge[61] program was

used to compile molecular orbital contributions from the single-point calculations.

X-Ray Crystal Structure Analyses

Data of **10** were collected using a Bruker Quest CMOS diffractometer with Mo-Kα radiation (λ = 0.71073 Å). Data of **6C**, **7A**, **8** and **9** were collected using a Bruker AXS X8 Prospector CCD diffractometer with Cu-Kα radiation (λ = 1.54178 Å). The instruments were equipped with IμS microsources with a laterally graded multilayer (Goebel) mirrors for monochromatization and with Oxford Cryosystems low temperature devices. Single crystals were mounted on Mitegen micromesh mounts using a trace of mineral oil and cooled in-situ to 100(2) K for data collection. Data were collected, reflections were indexed and processed, and the files scaled and corrected for absorption using APEX2 and SADABS or TWINABS. The space groups were assigned and the structures were solved by direct methods using XPREP within the SHELXTL suite of programs and refined by full matrix least squares against F^2 with all reflections using Shelxl2013 using the graphical interface Shelxle.[62]

If not specified otherwise H atoms attached to carbon, boron and nitrogen atoms as well as hydroxyl hydrogens were positioned geometrically and constrained to ride on their parent atoms. C-H bond distances were constrained to 0.95 Å for aromatic and alkene C-H moieties, and to 0.99 and 0.98 Å for aliphatic CH_2 and CH_3 moieties, respectively. N-H bond distances were constrained to 0.88 Å for planar (sp^2 hybridized) N-H groups. Methyl CH_3 H atoms were allowed to rotate but not to tip to best fit the experimental electron density. U_{iso}(H) values were set to a multiple of U_{eq}(C/N/O) with 1.5 for CH_3 and OH, and 1.2 for C-H, CH_2 and N-H units, respectively.

Key crystal structure and refinement data for dioxochlorins isomers **6**–**10** are provided in Table 4. Details of the data collection and structural parameters for the structure elucidation, descriptions of disorder and hydrogen atom treatment, and software packages used, can also be found in the ESI.

Table 4. Crystal structure and refinement data for dioxochlorins isomers **6**–**10**.[a]

Head 1[a]	**6**	**7**	**8**	**9**	**10**
empirical formula	$C_{36}H_{46}N_4O_2$	$C_{75}H_{99}N_8O_4$	$C_{36}H_{46}N_4O_2$	$C_{36}H_{46}N_4O_2$	$C_{36}H_{46}N_4O_2$
formula weight	566.77	1176.62	566.77	566.77	566.77
crystal size [mm³]	0.14 × 0.12 × 0.10	0.26 × 0.22 × 0.04	0.41 × 0.26 × 0.19	0.07 × 0.04 × 0.01	0.55 × 0.15 × 0.08
crystal system	Monoclinic	Triclinic	Monoclinic	Triclinic	Monoclinic
space group	$P2_1/n$	$P\bar{1}$	$P2_1/c$	$P\bar{1}$	$P2_1/n$
a, *b*, *c* [Å]	8.142 (2), 22.128 (6), 17.692 (4)	10.6513 (7), 18.5944 (11), 19.0109 (11)	9.9015 (5), 12.3381 (7), 25.0912 (12)	9.826 (2), 12.957 (3), 13.040 (3)	17.6467 (7), 15.1535 (5), 24.838 (1)
α, β, γ [°]	90, 96.427 (18), 90	87.039 (3), 84.070 (4), 82.506 (4)	90, 98.878 (2), 90	69.915 (10), 88.994 (10), 85.649 (10)	90, 99.309 (1), 90
V [Å³]	3167.4 (15)	3710.3 (4)	3028.6 (3)	1554.7 (6)	6554.4 (4)
Z	4	2	4	2	8
ρ [Mg/m³]	1.189	1.053	1.243	1.211	1.149
F(000)	1224	1274	1224	612	2448
μ [mm^{-1}]	0.58	0.51	0.60	0.59	0.07
T_{min}, T_{max}	0.452, 0.753	0.456, 0.753	0.620, 0.753	0.669, 0.753	0.702, 0.745
θ-range [°]	3.2–67.3	2.4–66.9	3.6–67.0	3.6–66.3	2.3–25.7
hkl-range	h = -9 → 9, k = 0 → 26, l = 0 → 20	h = -12 → 12, k = -21 → 22, l = -22 → 22	h = -10 → 11, k = -14 → 14, l = -29 → 29	h = -11 → 11, k = -14 → 15, l = -15 → 15	h = -21 → 21, k = -18 → 17, l = -30 → 30
collected refl.	5568	37789	29260	16472	53513
Independent reflections	5568	12779	5344	5378	12419
obs. refl. ($I > 2\sigma(I)$)	4249	7489	5190	4328	10083
data / restraints / parameters	5568 / 63 / 430	12779 / 70 / 831	5344 / 0 / 388	5378 / 0 / 387	12419 / 0 / 773
Completeness	to θ = 67.679° (95.6 %)	to θ = 67.118° (96.3%)	to θ = 67.155° (98.8 %)	to θ = 67.012° (96.8 %)	to θ = 25.696° (99.6 %)
goodness-of-fit (F^2)	1.09	0.96	1.06		1.04

*R*1, *wR*2 ($I > 2\sigma(I)$)	0.102	0.080	0.036	0.040	0.042
*R*1, *wR*2 (all data)	0.296	0.205	0.090	0.111	0.103
residual electron density [e/Å³]	0.33, -0.32	0.59, -0.30	0.28, -0.21	0.22, -0.20	0.29, -0.21
CCDC #	1994809	1994810	1994811	1994812	1994813

[a] For software used, see ESI.

CCDC-1994809 (**6**), CCDC-1994810 (**7**), CCDC-1994811 (**8**), CCDC-1994812 (**9**), and CCDC-1994813 (**10**) contain the supplementary crystallographic data for this paper and can be obtained free of charge from The Cambridge Crystallographic Data Centre via www.ccdc.cam.ac.uk/data_request/cif.

Acknowledgements

Funding for this work was provided by the U.S. National Science Foundation (NSF) through grants CHE-1465133 and CHE-1800631 (to CB). The APEX II CCD X-ray diffractometer was funded by NSF Grant CHE-0087210, Ohio Board of Regents Grant CAP-491, and by Youngstown State University; the Quest CMOS X-ray diffractometer was funded by NSF Grant CHE-1625543 (MZ). AAPC, AG and SB are thankful for U.K.'s Engineering and Physical Sciences Research Council (EPSRC) grants EP/R045305/1 and EP/R042802/1.

We thank David Dolphin, University of British Columbia, and Chi-Kwong (Chris) Chang, Michigan State University, for a donation of the **OEP** used in this study.

Keywords: octaalkylporphyrins • β-oxoporphyrinoids • bacteriochlorins • isobacteriochlorins • electronic structure

[1] A. R. Battersby, *Nat. Prod. Rep.* **2000**, *17*, 507–526.

[2] M. Grinstein, *J. Biol. Chem.* **1947**, *167*, 515–519.

[3] Y. Shioi, in *Chlorophylls and Bacteriochlorophylls* (Eds.: B. Grimm, R. J. Porra, W. Rüdiger, H. Scheer), Springer, Dordrecht, NL, **2006**, pp. 123–131.

[4] a) K. M. Smith, *Acc. Chem. Res.* **1979**, *12*, 374–381; b) H. Scheer, H. H. Inhoffen, in *The Porphyrins, Vol. 2* (Ed.: D. Dolphin), Academic Press, New York, **1978**, pp. 45–90; c) W. Flitsch, *Adv. Heterocycl. Chem.* **1988**, *43*, 73–126; d) F.-P. Montforts, B. Gerlach, F. Höper, *Chem. Rev.* **1994**, *94*, 327–347; e) R. Yerushalmi, I. Ashur, A. Scherz, in *Chlorophylls and Bacteriochlorophylls* (Eds.: B. Grimm, R. J. Porra, W. Rüdiger, H. Scheer), Springer, Dordrecht, NL, **2006**, pp. 495–506; f) M. Galezowski, D. T. Gryko, *Curr. Org. Chem.* **2007**, *11*, 1310–1338; g) W. G. O'Neal, P. A. Jacobi, *J. Am. Chem. Soc.* **2008**, *130*, 1102–1108; h) C. Brückner, L. Samankumara, J. Ogikubo, in *Handbook of Porphyrin Science, Vol. 17* (Eds.: K. M. Kadish, K. M. Smith, R. Guilard), World Scientific, River Edge, NY, **2012**, pp. 1–112; i) J. S. Lindsey, *Chem. Rev.* **2015**, *115*, 6534–6620; j) M. Taniguchi, J. S. Lindsey, *Chem. Rev.* **2017**, *117*, 344–535; k) Y. Liu, S. Zhang, J. S. Lindsey, *Natural Product Reports* **2018**, *35*, 879–901; l) Y. Liu, J. S. Lindsey, *J. Org. Chem.* **2016**, *81*, 11882–11897; m) S. Zhang, H.-J. Kim, Q. Tang, E. Yang, D. F. Bocian, D. Holten, J. S. Lindsey, *New J. Chem.* **2016**, *40*, 5942–5956.

[5] a) M. Liu, C.-Y. Chen, D. Hood, M. Taniguchi, J. R. Diers, D. F. Bocian, D. Holten, J. S. Lindsey, *New J. Chem.* **2017**, *41*, 3732–3744 ; b) D. Hood, D. M. Niedzwiedzki, R. Zhang, Y. Zhang, J. Dai, E. S. Miller, D. F. Bocian, P. G. Williams, J. S. Lindsey, D. Holten, *Photochem. Photobiol.* **2017**, *93*, 1204–1215; c) M. Taniguchi, H.-J. Kim, D. Ra, J. K. Schwartz, C. Kirmaier, E. Hindin, J. R. Diers, S. Prathapan, D. F. Bocian, D. Holten, J. S. Lindsey, *J. Org. Chem.* **2002**, *67*, 7329–7342.

[6] a) J. B. Paine, III, W. B. Kirshner, D. W. Moskowitz, D. Dolphin, *J. Org. Chem.* **1976**, *41*, 3857–3860; b) C. B. Wang, C. K. Chang, *Synthesis* **1979**, 548–549; c) J. L. Sessler, A. Mozaffari, M. R. Johnson, *Org. Synth.* **1992**, *70*, 68–78.

[7] OEP is also commercially available from a variety of chemical supply houses.

[8] a) M. d. G. H. Vicente, K. M. Smith, *Curr. Org. Synth.* **2014**, *11*, 3–28; b) R. Li, M. Zeller, C. Brückner, *Eur. J. Org. Chem.* **2017**, *2017*, 1820–1825; c) R. Li, M. Zeller, T. Bruhn, C. Brückner, *Eur. J. Org. Chem.* **2017**, *2017*, 1835–1842; d) K. R. Adams, R. Bonnett, P. J. Burke, A. Salgado, M. A. Valles, *J. Chem. Soc., Perkin Trans. 1* **1997**, 1769–1772; e) K. R. Adams, R. Bonnett, P. J. Burke, A. Salgado, M. A. Valles, *J. Chem. Soc., Chem. Commun.* **1993**, 1860–1861; f) C. Ryppa, D. Niedzwiedzki, N. L. Morozowich, R. Srikanth, M. Zeller, H. A. Frank, C. Brückner, *Chem.—Eur. J.* **2009**, *15*, 5749–5762; g) M. Sharma, E. Meehan, B. Q. Mercado, C. Brückner, *Chem.—Eur. J.* **2016**, *22*, 11706–11718; h) R. Li, E. Meehan, M. Zeller, C. Brückner, *Eur. J. Org. Chem.* **2017**, *2017*, 1826–1834.

[9] a) K. M. Kadish, W. E, R. Zhan, T. Khoury, L. J. Govenlock, J. K. Prashar, P. J. Sintic, K. Ohkubo, S. Fukuzumi, M. J. Crossley, *J. Am. Chem. Soc.* **2007**, *129*, 6576–6588; b) M. J. Crossley, L. J. Govenlock, J. K. Prashar, *J. Chem. Soc., Chem. Commun.* **1995**, 2379–2380; c) C. Brückner, J. R. McCarthy, H. W. Daniell, Z. D. Pendon, R. P. Ilagan, T. M. Francis, L. Ren, R. R. Birge, H. A. Frank, *Chem. Phys.* **2003**, *294*, 285–303; d) M. Taniguchi, M. N. Kim, D. Ra, J. S. Lindsey, *J. Org. Chem.* **2005**, *70*, 275–285; e) P. Vairaprakash, E. Yang, T. Sahin, M. Taniguchi, M. Krayer, J. R. Diers, A. Wang, D. M. Niedzwiedzki, C. Kirmaier, J. S. Lindsey, D. F. Bocian, D. Holten, *J. Phys. Chem. B* **2015**, *119*, 4382–4395; f) D. Schnable, N. Chaudhri, R. Li, M. Zeller, C. Brückner, *Inorg. Chem.* **2020**, *59*, 2870−2880.

[10] M. E. Alberto, B. C. De Simone, E. Sicilia, M. Toscano, N. Russo, *Int. J. Mol. Sci.* **2019**, *20*, 2002.

[11] a) C. Brückner, J. Ogikubo, J. R. McCarthy, J. Akhigbe, M. A. Hyland, P. Daddario, J. L. Worlinsky, M. Zeller, J. T. Engle, C. J. Ziegler, M. J. Ranaghan, M. N. Sandberg, R. R. Birge, *J. Org. Chem.* **2012**, *77*, 6480–6494; b) X. S. Ke, B. Y. Yang, X. Cheng, L. F. Chan Sharon, J. L. Zhang, *Chem.–Eur. J.* **2014**, *20*, 4324–4333; c) N. Hewage, P. Daddario, K. S. F. Lau, M. J. Guberman-Pfeffer, J. A. Gascón, M. Zeller, C. O. Lee, G. E. Khalil, M. Gouterman, C. Brückner, *J. Org. Chem.* **2019**, *84*, 239–256; d) M. J. Guberman-Pfeffer, R. F. Lalisse, N. Hewage, C. Brückner, J. A. Gascón, *J. Phys. Chem. A* **2019**, *123*, 7470–7485; e) Y. Ning, G.-Q. Jin, J.-L. Zhang, *Acc. Chem. Res.* **2019**, *52*, 2620–2633; f) C. Brückner, A. O. Atoyebi, D. Girouard, K. S. F. Lau, J. Akhigbe, L. Samankumara, D. Damunupola, G. E. Khalil, M. Gouterman, J. A. Krause, M. Zeller, *Eur. J. Org. Chem.* **2020**, *2020*, 475–482.

[12] Y. Yao, Y. Rao, Y. Liu, L. Jiang, J. Xiong, Y. J. Fan, Z. Shen, J. L. Sessler, J. L. Zhang, *Phys. Chem. Chem. Phys.* **2019**, *21*, 10152–10162.

[13] a) C. K. Chang, *J. Biol. Chem.* **1985**, *260*, 9520–9522; b) C. K. Chang, W. Wu, *J. Biol. Chem.* **1986**, *261*, 8593–8596; c) C. K. Chang, R. Timkovich, W. Wu, *Biochemistry* **1986**, *25*, 8447–8453.

[14] a) M. R. Prinsep, T. G. Appleton, G. R. Hanson, I. Lane, C. D. Smith, J. Puddick, D. P. Fairlie, *Inorg. Chem.* **2017**, *56*, 5577–5585; b) M. R. Prinsep, G. M. L. Patterson, L. K. Larsen, C. D. Smith, *J. Nat. Prod.* **1998**, *61*, 1133–1136; c) C. D. Smith, M. R. Prinsep, F. R. Caplan, R. E. Moore, G. M. L. Patterson, *Oncol. Res.* **1994**, *6*, 211–218; d) M. R. Prinsep, F. R. Caplan, R. E. Moore, G. M. L. Patterson, C. D. Smith, *J. Am. Chem. Soc.* **1992**, *114*, 385–387; e) C. Brückner, *Photochem. Photobiol.* **2017**, *93*, 1320–1325.

[15] a) K. M. Barkigia, C. K. Chang, J. Fajer, M. W. Renner, *J. Am. Chem. Soc.* **1992**, *114*, 1701–1707; b) C. K. Chang, K. M. Barkigia, L. K. Hanson, J. Fajer, *J. Am. Chem. Soc.* **1986**, *108*, 1352–1354.

[16] a) H. Fischer, H. Orth, *Die Chemie des Pyrrols, Vol. II, Part I*, Akademische Verlagsgesellschaft (Johnson Reprint, New York 1968), Leipzig, **1937**; b) H. Fischer, H. Gebhardt, A. Rothhaas, *Liebigs Ann. Chem.* **1930**, *482*, 1–24.

[17] a) R. Bonnett, D. Dolphin, A. W. Johnson, D. Oldfield, G. F. Stephenson, *Proc. Chem. Soc.* **1964**, 371–372; b) R. Bonnett, M. J. Dimsdale, G. F. Stephenson, *J. Chem. Soc. C* **1969**, 564–570.

[18] a) H. H. Inhoffen, W. Nolte, *Justus Liebigs Ann. Chem.* **1969**, *725*, 167–176; b) C. K. Chang, *Biochemistry* **1980**, *19*, 1971–1976; c) H. H. Inhoffen, W. Nolte, *Tetrahedron Lett.* **1967**, *8*, 2185–2187.

[19] a) C. K. Chang, C. Sotiriou, *J. Heterocycl. Chem.* **1985**, *22*, 1739–1741; b) H. Fischer, H. Pfeiffer, *Liebigs Ann. Chem.* **1944**, *556*, 131–153.

[20] C. K. Chang, W. Wu, *J. Org. Chem.* **1986**, *51*, 2134–2137.

[21] a) A. M. Stolzenberg, P. A. Glazer, B. M. Foxman, *Inorg. Chem.* **1986**, *25*, 983–991; b) A. M. Stolzenberg, M. T. Stershic, *Inorg. Chem.* **1987**, *26*, 3082–3083; c) A. M. Stolzenberg, M. T. Steshic, *J. Am. Chem. Soc.* **1988**, *110*, 6391–6402; d) R. Bonnett, A. N. Nizhnik, M. C. Berenbaum, *J. Chem. Soc., Chem. Commun.* **1989**, 1822–1823.

[22] A. M. Stolzenberg, S. W. Simerly, B. D. Steffey, G. S. Haymond, *J. Am. Chem. Soc.* **1997**, *119*, 11843–11854.

[23] A. M. Stolzenberg, M. A. Laliberte, *J. Org. Chem.* **1987**, *52*, 1022–1027.

[24] K. R. Adams, M. C. Berenbaum, R. Bonnett, A. N. Nizhnik, A. Salgado, M. A. Valles, *J. Chem. Soc., Perkin Trans. 1* **1992**, 1465–1470.

[25] R. D. Arasasingham, A. L. Balch, M. M. Olmstead, *Heterocycles* **1988**, *27*, 2111–2118.

[26] E. Meehan, R. Li, M. Zeller, C. Brückner, *Org. Lett.* **2015**, *17*, 2210–2213.

[27] F. Tutunea, M. D. Ryan, *J. Electroanal. Chem.* **2012**, *670*, 16–22.

[28] T. J. Neal, S.-J. Kang, C. E. Schulz, W. R. Scheidt, *Inorg. Chem.* **1999**, *38*, 4294–4302.

[29] T. J. Neal, S.-J. Kang, I. Turowska-Tyrk, C. E. Schulz, W. R. Scheidt, *Inorg. Chem.* **2000**, *39*, 872–880.

[30] S. Cai, E. Belikova, L. A. Yatsunyk, A. M. Stolzenberg, F. A. Walker, *Inorg. Chem.* **2005**, *44*, 1882–1889.

[31] D. B. Papkovsky, G. V. Ponomarev, W. Trettnak, P. O'Leary, *Anal. Chem.* **1995**, *67*, 4112–4117.

[32] a) P. A. Connick, K. A. Macor, *Inorg. Chem.* **1991**, *30*, 4654–4663; b) P. A. Connick, K. J. Haller, K. A. Macor, *Inorg. Chem.* **1993**, *32*, 3256–3264.

[33] N. Chaudhri, M. Zeller, C. Brückner, *J. Org. Chem.* **2020**, *85*, 13951–13964.

[34] C. J. Kingsbury, M. O. Senge, *Coord. Chem. Rev.* **2021**, *431*, 213760.

[35] J. W. Lauher, J. A. Ibers, *J. Am. Chem. Soc.* **1973**, *95*, 5148–5152.

[36] T. Bruhn, C. Brückner, *J. Org. Chem.* **2015**, *80*, 4861–4868.

[37] X.-S. Ke, Y. Chang, J.-Z. Chen, J. Tian, J. Mack, X. Cheng, Z. Shen, J.-L. Zhang, *J. Am. Chem. Soc.* **2014**, *136*, 9598–9607.

[38] W. Jentzen, X.-Z. Song, J. A. Shelnutt, *J. Phys. Chem. B.* **1997**, *101*, 1684–1699.

[39] M. Stepien, L. Latos-Grazynski, *Top. Heterocycl. Chem.* **2009**, *19*, 83–153.

[40] M. Gouterman, in *The Porphyrins, Vol. 3* (Ed.: D. Dolphin), Academic Press, New York, **1978**, pp. 1–165.

[41] M. Taniguchi, J. S. Lindsey, D. F. Bocian, D. Holten, *J. Photochem. Photobiol., C* **2021**, *46*, 100401.

[42] F. Wilkinson, W. P. Helman, A. B. Ross, *J. Phys. Chem. Ref. Data* **1993**, *22*, 113–262.

[43] J. Mack, *Chem. Rev.* **2017**, *117*, 3444–3478.

[44] S. Sripothongnak, C. J. Ziegler, M. R. Dahlby, V. N. Nemykin, *Inorg. Chem.* **2011**, *50*, 6902–6909.

[45] M. Gouterman, *J. Mol. Spectrosc.* **1961**, *6*, 138–163.

[46] M. Umetsu, Z.-Y. Wang, M. Kobayashi, T. Nozawa, *Biochim. Biophys. Acta, Bioenerg.* **1999**, *1410*, 19–31.

[47] a) B. Briat, D. A. Schooley, R. Records, E. Bunnenberg, C. Djerassi, *J. Am. Chem. Soc.* **1967**, *89*, 6170–6177; b) J. D. Keegan, A. M. Stolzenberg, Y.-C. Lu, R. E. Linder, G. Barth, E. Bunnenberg, C. Djerassi, A. Moscowitz, *J. Am. Chem. Soc.* **1981**, *103*, 3201–3203; c) J. D. Keegan, A. M. Stolzenberg, Y. C. Lu, R. E. Linder, G. Barth, A. Moscowitz, E. Bunnenberg, C. Djerassi, *J. Am. Chem. Soc.* **1982**, *104*, 4317–4329; d) J. D. Keegan, A. M. Stolzenberg, Y. C. Lu, R. E. Linder, G. Barth, A. Moscowitz, E. Bunnenberg, C. Djerassi, *J. Am. Chem. Soc.* **1982**, *104*, 4305–4317; e) W. Y. Huang, U. P. Wild, L. W. Johnson, *J. Phys. Chem.* **1992**, *96*, 6189–6195; f) A. M. Huff, C. K. Chang, D. K. Cooper, K. M. Smith, J. H. Dawson, *Inorg. Chem.* **1993**, *32*, 1460–1466; g) A. M. Bracete, S. Kadkhodayan, M. Sono, A. M. Huff, C. Zhuang, D. K. Cooper, K. M. Smith, C. K. Chang, J. H. Dawson, *Inorg. Chem.* **1994**, *33*, 5042–5049; h) Y. Nonomura, S. Igarashi, N. Yoshioka, H. Inoue, *Chem. Phys* **1997**, 155–166; i) J. Mack, Y. Asano, N. Kobayashi, M. J. Stillman, *J. Am. Chem. Soc.* **2005**, *127*, 17697–17711; j) J. C. J. M. D. S. Menezes, M. A. F. Faustino, K. T. de Oliveira, M. P. Uliana, V. F. Ferreira, S. Hackbarth, B. Röder, T. Teixeira Tasso, T. Furuyama, N. Kobayashi, A. M. S. Silva, M. G. P. M. S. Neves, J. A. S. Cavaleiro, *Chem. – Eur. J.* **2014**, *20*, 13644–13655.

[48] a) R. V. Belosludov, D. Nevonen, H. M. Rhoda, J. R. Sabin, V. N. Nemykin, *J. Phys. Chem. A* **2019**, *123*, 132–152; b) V. N. Nemykin, R. G. Hadt, R. V. Belosludov, H. Mizuseki, Y. Kawazoe, *J. Phys. Chem. A* **2007**, *111*, 12901–12913; c) A. G. Martynov, J. Mack, A. K. May, T. Nyokong, Y. G. Gorbunova, A. Y. Tsivadze, *ACS Omega* **2019**, *4*, 7265–7284.

[49] H. M. Rhoda, J. Akhigbe, J. Ogikubo, J. R. Sabin, C. J. Ziegler, C. Brückner, V. N. Nemykin, *J. Phys. Chem. A* **2016**, *120*, 5805–5815.

[50] a) R. W. Redmond, J. N. Gamlin, *Photochem. Photobiol.* **1999**, *70*, 391–475; b) R. K. Pandey, G. Zheng, in *The Porphyrin Handbook, Vol. 6* (Eds.: K. M. Kadish, K. M. Smith, R. Guilard), Academic Press, San Diego, **2000**, pp. 157–230.

[51] a) M. C. DeRosa, R. J. Crutchley, *Coord. Chem. Rev.* **2002**, *233–234*, 351–371; b) R. Bonnett, M. A. Krysteva, I. G. Lalov, S. V. Artarsky, *Water Res.* **2006**, *40*, 1269–1275.

[52] M. V. Appleby, P. G. Walker, D. Pritchard, S. van Meurs, C. M. Booth, C. Robertson, M. D. Ward, D. J. Kelly, J. A. Weinstein, *Mater. Adv.* **2020**, *1*, 3417–3427.

[53] a) W. R. Mason, *A Practical Guide to Magnetic Circular Dichroism Spectroscopy*, John Wiley & Sons, Inc, Hoboken, NJ, **2007**; b) J. Mack, N. Kobayashi, *Chem. Rev.* **2011**, *111*, 281–321; c) N. Kobayashi, A. Muranaka, J. Mack, *Circular Dichroism and Magnetic Circular Dichroism Spectroscopy for Organic Chemists*, RSC, London, **2012**.

[54] M. J. Frisch, G. W. Trucks, H. B. Schlegel, G. E. Scuseria, M. A. Robb, J. R. Cheeseman, G. Scalmani, V. Barone, B. Mennucci, G. A. Petersson, H. Nakatsuji, M. Caricato, X. Li, H. P. Hratchian, A. F. Izmaylov, J. Bloino, G. Zheng, J. L. Sonnenberg, M. Hada, M. Ehara, K. Toyota, R. Fukuda, J. Hasegawa, M. Ishida, T. Nakajima, Y. Honda, O. Kitao, H. Nakai, T. Vreven, J. A. Montgomery Jr., J. E. Peralta, F. Ogliaro, M. J. Bearpark, J. Heyd, E. N. Brothers, K. N. Kudin, V. N. Staroverov, R. Kobayashi, J. Normand, K. Raghavachari, A. P. Rendell, J. C. Burant, S. S. Iyengar, J. Tomasi, M. Cossi, N. Rega, N. J. Millam, M. Klene, J. E. Knox, J. B. Cross, V. Bakken, C. Adamo, J. Jaramillo, R. Gomperts, R. E. Stratmann, O. Yazyev, A. J. Austin, R. Cammi, C. Pomelli, J. W. Ochterski, R. L. Martin, K. Morokuma, V. G. Zakrzewski, G. A. Voth, P. Salvador, J. J. Dannenberg, S. Dapprich, A. D. Daniels, Ö. Farkas, J. B. Foresman, J. V. Ortiz, J. Cioslowski, D. J. Fox, Gaussian, Inc., Wallingford, CT, USA, **2009**.

[55] a) A. D. Becke, *Phys. Rev. A* **1988**, *38*, 3098–3100; b) J. P. Perdew, *Phys. Rev. B* **1986**, *33*, 8822–8824.

[56] R. Peverati, D. G. Truhlar, *Phys. Chem. Chem. Phys.* **2012**, *14*, 13171–13174.

[57] J. M. Tao, J. P. Perdew, V. N. Staroverov, G. E. Scuseria, *Phys. Rev. Lett.* **2003**, *91*, 146401/146401–146401/146404.

[58] Y. Zhao, D. G. Truhlar, *Theor. Chem. Acc.* **2008**, *120*, 215–241.

[59] A. D. McLean, G. S. Chandler, *J. Chem. Phys.* **1980**, *72*, 5639–5648.

[60] J. Tomasi, B. Mennucci, R. Cammi, *Chem. Rev.* **2005**, *105*, 2999–3093.

[61] A. L. Tenderholt, 2.1 ed., Stanford University, Stanford, CA, **2011**.

[62] G. M. Sheldrick, *Acta Crystallogr. Sect. A* **2008**, *64*, 112–122.

Entry for the Table of Contents

The single crystal structures of all octaethyl-β,β'-dioxo isomers and a description of their UV-vis absorption spectra in neutral and acidic solutions, fluorescence emission properties, MCD spectra, and their singlet oxygen photosensitization properties is presented. DFT Computations reveal the underlying tautomeric equilibria and the strong electronic interactions of the β-oxofunctionalities with the porphyrinic π-system.